

SUSY Higgs Boson Decays into Scalar Quarks: QCD Corrections

A. ARHRIB^{1,2}, A. DJOUADI¹, W. HOLLIK³ and C. JÜNGER³

¹ Laboratoire de Physique Mathématique et Théorique, UPRES-A 5032,
Université de Montpellier II, F-34095 Montpellier Cedex 5, France.

² Laboratoire de Physique et Techniques Nucléaires
Faculté des Sciences Semlalia, B. P S15, Marrakech Morocco.

³ Institut für Theoretische Physik, Universität Karlsruhe,
D-76128 Karlsruhe, Germany.

Abstract

In supersymmetric theories, the decays of the neutral CP-even and CP-odd as well as the charged Higgs bosons into scalar quarks, in particular into top and bottom squarks, can be dominant if they are kinematically allowed. We calculate the QCD corrections to these decay modes in the minimal supersymmetric extension of the Standard Model, including all quark mass terms and squark mixing. These corrections turn out to be rather large, altering the decay widths by an amount which can be larger than 50%. The corrections can be either positive or negative, and depend strongly on the mass of the gluino. We also discuss the QCD corrections to the decays of heavy scalar quarks into light scalar quarks and Higgs bosons.

1. Introduction

Supersymmetric theories [1] are widely considered as the most attractive extensions of the Standard Model. In a grand unified framework, they protect scalar Higgs bosons from acquiring very large masses and provide the opportunity to generate the electroweak symmetry breaking radiatively. In the minimal version of these theories, the Minimal Supersymmetric Standard Model (MSSM), the Higgs sector is extended to contain two doublet fields, leading to five physical states [2]: two CP-even neutral Higgs bosons, h and H , a CP-odd Higgs boson A and two charged Higgs particles H^\pm . While the lightest CP-even Higgs boson h mass is predicted to be less than 130 GeV [3], the H , A and H^\pm states are expected to have masses of order of the electroweak symmetry breaking scale.

If all genuine SUSY particles are very heavy, the neutral and charged Higgs bosons will decay into standard fermions and gauge bosons, as well as into cascades involving the lighter Higgs bosons; in most cases the decays into heavy b and t quark pairs are dominant. These decay modes have been extensively discussed in the literature and for a recent summary we refer the reader to Ref. [4]. However, it could well be that charginos, neutralinos and sfermions are light enough for the Higgs decays into these particles to be kinematically allowed. For instance, in grand unified models with proper radiative electroweak symmetry breaking, the H , A and H^\pm bosons are rather heavy and approximately mass degenerate, $M_H \simeq M_A \simeq M_{H^\pm} \sim$ a few hundred GeV, while charginos, neutralinos and eventually top and bottom squarks have masses of $\mathcal{O}(100 \text{ GeV})$ [5]. In this case, the decay pattern of the heavy Higgs particles H , A and H^\pm will be drastically different [6, 7]. In particular, because of the large Yukawa couplings and large squark mixing, the decays of the heavy Higgs bosons into top and bottom squarks can be competitive with the standard decay channels and can even be the dominant ones in some areas of the MSSM parameter space [7].

It is well known that the standard hadronic decay modes of Higgs particles are significantly affected by QCD radiative corrections [8]. In order to have full control on the Higgs decay widths into squark pairs – and to make a reliable comparison with the standard decays – QCD corrections have also to be included. Recently, the QCD corrections to the decay of the charged Higgs boson into $\tilde{t}\tilde{b}$ pairs have been calculated [9] and found to be quite substantial.

In the present paper, we derive the QCD corrections to the decays of the neutral CP-even and CP-odd Higgs bosons into stop and sbottom pairs. These corrections are found to be rather large, altering the Born decay widths by an amount which can exceed 50%. These effects must therefore be taken into account. We also rederive the QCD corrections to the decays of the charged Higgs boson into $\tilde{t}\tilde{b}$ pairs using a different [and more convenient] renormalization scheme compared to the one adopted in Ref. [9]. We find that the corrections can be extremely large and can strongly suppress the decay width compared to its tree-level value. Finally, we also discuss for completeness the QCD corrections to the reverse decay of heavy squarks into their lighter partners plus light Higgs bosons; these decays have been discussed at tree-level in Ref. [10].

The paper is organized as follows: to set the notation and to introduce the various parameters which enter the analysis, we summarize in the next section the Higgs decay widths into squark pairs in Born approximation. In section 3, we present the analytic expressions of the QCD corrections to the decay widths. Section 4 contains the discussion of the numerical results. In section 5, we discuss the QCD corrections to the decays of heavy squarks into Higgs bosons and we give our conclusions in section 6.

2. Born Approximation

The amplitudes for the decay widths of the MSSM neutral heavy CP-even, CP-odd and charged Higgs bosons¹, that we will collectively denote by Φ , into the scalar partners of first and second generation quarks

$$\Phi \rightarrow \tilde{q}_i \bar{\tilde{q}}_j \quad , \quad \Phi = H, A, H^\pm \quad (1)$$

depend on three parameters if the quark mass is neglected: the mass of the decaying Higgs boson, the squark masses [more precisely the left- and right-handed soft SUSY breaking scalar masses $m_{\tilde{q}_L}$ and $m_{\tilde{q}_R}$, which in general are taken to be equal] and the ratio of the vacuum expectation values of the two MSSM Higgs fields $\tan \beta$. A mixing angle α in the CP-even Higgs sector also enters the amplitudes, but in the MSSM it can be expressed in terms of $\tan \beta$ and the Higgs boson mass M_Φ .

In the case of the third generation scalar quarks, and in particular top squarks, the mixing between left- and right-handed squarks, which is proportional to the mass of the partner quark, must be included [12]. In terms of the scalar masses $m_{\tilde{q}_L}, m_{\tilde{q}_R}$, the Higgs-higgsino mass parameter μ and the soft SUSY-breaking trilinear coupling A_q , the squark mass matrices read

$$\begin{aligned} \mathcal{M}_{\tilde{q}}^2 &= \begin{pmatrix} m_q^2 + M_{LL}^2 & m_q M_{LR} \\ m_q M_{LR} & m_q^2 + M_{RR}^2 \end{pmatrix} \\ M_{LL}^2 &= m_{\tilde{q}_L}^2 + (I_3^q - e_q s_W^2) \cos 2\beta M_Z^2 \\ M_{RR}^2 &= m_{\tilde{q}_R}^2 + e_q s_W^2 \cos 2\beta M_Z^2 \\ M_{LR} &= A_q + \mu (\tan \beta)^{-2I_3^q} . \end{aligned} \quad (2)$$

I_3^q and e_q are the weak isospin and electric charge of the squark \tilde{q} , and $s_W^2 = 1 - c_W^2 \equiv \sin^2 \theta_W$. They are diagonalized by the 2×2 rotation matrices

$$R^{\tilde{q}} = \begin{pmatrix} c_{\theta_q} & -s_{\theta_q} \\ s_{\theta_q} & c_{\theta_q} \end{pmatrix} \quad , \quad c_{\theta_q} \equiv \cos \theta_q \quad \text{and} \quad s_{\theta_q} \equiv \sin \theta_q \quad (3)$$

¹In view of the experimental bounds on the squark masses [11], the lightest CP-even Higgs boson in the MSSM cannot decay into squark pairs since its maximal mass value is smaller than $M_h \lesssim 130$ GeV [3]. These decays will therefore not be considered here. However, the analytical expressions can be straightforwardly obtained from the decays of the heavy CP-even Higgs boson, after the proper changes in the Higgs boson couplings.

which turn the mass eigenstates, \tilde{q}_1 and \tilde{q}_2 , into the current eigenstates \tilde{q}_L and \tilde{q}_R ; the mixing angle and squark masses are then given by

$$\tan \theta_q = \frac{2 m_q M_{LR}}{M_{LL}^2 - M_{RR}^2 - \sqrt{(M_{LL}^2 - M_{RR}^2)^2 + 4 m_q^2 M_{LR}^2}} \quad (4)$$

and

$$m_{\tilde{q}_{1,2}}^2 = m_q^2 + \frac{1}{2} \left[M_{LL}^2 + M_{RR}^2 \mp \sqrt{(M_{LL}^2 - M_{RR}^2)^2 + 4 m_q^2 M_{LR}^2} \right] \quad (5)$$

In the Born approximation, the decay widths of the MSSM heavy CP-even, CP-odd and charged Higgs bosons into squark pairs, eq. (1), can be written as [13]

$$\Gamma^0(\Phi \rightarrow \tilde{q}_i \bar{\tilde{q}}'_j) = \frac{3G_F}{4\sqrt{2}\pi M_\Phi^3} \lambda^{1/2}(M_\Phi^2, m_{\tilde{q}_i}^2, m_{\tilde{q}'_j}^2) (G_{\Phi ij})^2 \quad (6)$$

where $\lambda = x^2 + y^2 + z^2 - 2(xy + xz + yz)$ is the two-body phase space function. The couplings of the Higgs bosons to squarks $G_{\Phi ij}$ read

$$G_{\Phi ij} = \frac{1}{\sqrt{2}} \sum_{k,l=1}^2 (R^{\tilde{q}})_{ik}^T C_{\Phi \tilde{q}\tilde{q}'}^{kl} (R^{\tilde{q}'})_{lj} \quad (7)$$

with the matrices $C_{\Phi \tilde{q}\tilde{q}'}$ summarizing the couplings of the Higgs bosons to the squark current eigenstates; for the H, A and H^\pm particles, they are given by

$$C_{H\tilde{q}\tilde{q}} = \begin{pmatrix} (2I_3^q - 2e_q s_W^2) M_Z^2 \cos(\beta + \alpha) + 2m_q^2 r_1^q & m_q(A_q r_1^q + \mu r_2^q) \\ m_q(A_q r_1^q + \mu r_2^q) & 2e_q s_W^2 M_Z^2 \cos(\beta + \alpha) + 2m_q^2 r_1^q \end{pmatrix} \quad (8)$$

$$C_{A\tilde{q}\tilde{q}} = \begin{pmatrix} 0 & -m_q [\mu - A_q (\tan \beta)^{-2I_3^q}] \\ m_q [\mu - A_q (\tan \beta)^{-2I_3^q}] & 0 \end{pmatrix} \quad (9)$$

$$C_{H^\pm \tilde{t}\tilde{b}} = \sqrt{2} \begin{pmatrix} m_b^2 \tan \beta + m_t^2 / \tan \beta - M_W^2 \sin 2\beta & m_b (A_b \tan \beta - \mu) \\ m_t (A_t / \tan \beta - \mu) & 2 m_t m_b / \sin 2\beta \end{pmatrix} \quad (10)$$

with the coefficients $r_{1,2}^q$ as

$$r_1^t = \frac{\sin \alpha}{\sin \beta} \quad , \quad r_2^t = \frac{\cos \alpha}{\sin \beta} \quad , \quad r_1^b = \frac{\cos \alpha}{\cos \beta} \quad , \quad r_2^b = \frac{\sin \alpha}{\cos \beta} \quad . \quad (11)$$

In principle, for the Higgs boson masses and the mixing angle α , one has also to include the large radiative corrections [3] which grow as the fourth power of m_t and induce an additional dependence on μ and A_q at the subleading level. However for rather heavy Higgs bosons, $M_H \sim M_A \sim M_{H^\pm} \gg M_Z$, these corrections will not affect the decay

amplitudes: the decaying Higgs boson mass can be used as input parameter and the angle α will reduce anyway to the value $\alpha \rightarrow \beta - \pi/2$. In this case, the couplings of the CP-even Higgs boson will simplify to

$$C_{H\tilde{q}\tilde{q}} = \begin{pmatrix} (2I_3^q - 2e_q s_W^2) M_Z^2 \sin 2\beta \mp 2m_q^2 (\tan \beta)^{\mp 1} & \mp m_q [A_q (\tan \beta)^{\mp 1} - \mu] \\ \mp m_q [A_q (\tan \beta)^{\mp 1} - \mu] & 2e_q s_W^2 M_Z^2 \sin 2\beta \mp 2m_q^2 (\tan \beta)^{\mp 1} \end{pmatrix}$$

where the “−” is for up-type squarks and the “+” for down-type squarks. When the quark masses and the squark mixing angles are set to zero, as is the case for first and second generation squarks, the pseudoscalar Higgs boson cannot decay at tree-level into squark pairs since the $A\tilde{q}_i\tilde{q}_i$ coupling is zero by virtue of CP-invariance and the $A\tilde{q}_1\tilde{q}_2$ coupling is proportional to m_q .

The decay widths of the heavy neutral CP-even and the charged Higgs bosons into first and second generation squarks are proportional to

$$\Gamma^0 \sim G_F M_W^4 \sin^2 2\beta / M_\Phi$$

in the asymptotic regime $M_\Phi \gg m_{\tilde{q}}$. These decays are suppressed by the heavy Higgs mass and therefore cannot compete with the dominant decay modes into top and/or bottom quarks [and to charginos and neutralinos] for which the decay widths grow as M_Φ .

In contrast, for the decays involving top squarks, the partial widths up to mixing angle factors are proportional to

$$\Gamma^0 \sim G_F m_t^4 / (M_\Phi \tan^2 \beta) \quad \text{or/and} \quad G_F m_t^2 (\mu + A_t / \tan \beta)^2 / M_\Phi .$$

For small $\tan \beta$ values and not too heavy Higgs bosons, or for intermediate values of $\tan \beta$ and for μ and A_t values of the order of ~ 1 TeV, the partial decay widths into top squarks can be very large and can compete with, and even dominate over, the decay channels into top quarks [and into charginos/neutralinos]. Furthermore, decays into sbottom quarks can also be important for large values of $\tan \beta$ and A_b . We therefore focus in this paper on the Higgs boson decays into third generation squarks; however, since we give complete analytic expressions, the decay widths into first and second generation can straightforwardly be obtained by setting the quark masses and the squark mixing angles to zero.

3. QCD Corrections

The QCD corrections to the Higgs decays into scalar quarks, eq. (1), consist of virtual corrections, Figs.1a–d, and real corrections with an additional gluon emitted off the final squark states, Fig. 1e. The $\mathcal{O}(\alpha_s)$ virtual contributions can be split into contributions with gluon [1a] and gluino [1b] exchange in the $\Phi\tilde{q}\tilde{q}'$ vertex, the mixing contribution due to the off-diagonal self energies of the outgoing squarks [1d] and the quartic squark interaction contribution [1c]. These contributions have to be supplemented by the wave-function counterterms, and by a counterterm renormalizing the $\Phi\tilde{q}_i\tilde{q}'_j$ interaction.

The partial widths of the decays of the MSSM Higgs bosons into scalar quarks, eq. (1), at $\mathcal{O}(\alpha_s)$ can be written as

$$\Gamma^1(\Phi \rightarrow \tilde{q}_i \bar{\tilde{q}}_j) = \frac{G_F}{2\sqrt{2}\pi M_\Phi^3} \frac{\alpha_s}{\pi} \lambda^{1/2}(M_\Phi^2, m_{\tilde{q}_i}^2, m_{\tilde{q}_j}^2) G_{\Phi ij} \Delta_{\Phi ij} \quad (12)$$

with

$$\Delta_{\Phi ij} = \Delta_{\Phi ij}^V + \Delta_{\Phi ij}^{\text{CT}} + \Delta_{\Phi ij}^R. \quad (13)$$

The sum of the virtual and counterterm corrections, $\Delta_{\Phi ij}^V$ and $\Delta_{\Phi ij}^{\text{CT}}$, is ultraviolet finite, as it should be, but still infrared divergent. The calculation has been performed in the dimensional reduction scheme [14], which preserves supersymmetry at the one loop level. However, the results are the same in both the dimensional regularization [15] and dimensional reduction schemes if the quark mass counterterms, which are needed to renormalize the $\Phi \tilde{q} \tilde{q}'$ interaction, are shifted appropriately by a finite amount [16]. The infrared divergence, which is regulated by introducing a fictitious mass λ for the gluon, is cancelled after including the real corrections $\Delta_{\Phi ij}^R$.

3.1 Virtual Corrections

The $\mathcal{O}(\alpha_s)$ virtual corrections in eq. (13) can be decomposed in the following way,

$$\Delta_{\Phi ij}^V = \Delta_{\Phi ij}^g + \Delta_{\Phi ij}^{\text{mix}} + \Delta_{\Phi ij}^{4\tilde{q}} + \Delta_{\Phi ij}^{\tilde{g}} \quad (14)$$

with Δ^g , Δ^{mix} , $\Delta^{4\tilde{q}}$ and $\Delta^{\tilde{g}}$ the contributions from the diagrams with gluon exchange, squark mixing, the quartic squark interaction and the gluino exchange respectively.

The contribution from the gluon exchange in the $\Phi \tilde{q} \tilde{q}'$ vertex is given by

$$\begin{aligned} \Delta_{\Phi ij}^g = & G_{\Phi ij} \left[B_0(m_{\tilde{q}_i}^2, \lambda, m_{\tilde{q}_i}) + B_0(m_{\tilde{q}_j'}^2, \lambda, m_{\tilde{q}_j'}) - B_0(M_\Phi^2, m_{\tilde{q}_i}, m_{\tilde{q}_j'}) \right. \\ & \left. + 2(m_{\tilde{q}_i}^2 + m_{\tilde{q}_j'}^2 - M_\Phi^2) C_0(m_{\tilde{q}_i}^2, M_\Phi^2, m_{\tilde{q}_j'}^2; \lambda, m_{\tilde{q}_i}, m_{\tilde{q}_j'}) \right] \end{aligned} \quad (15)$$

with B_0 and C_0 the Passarino–Veltman scalar two- and three point functions], the expressions of which can be found in Ref. [17].

The contribution from the off-diagonal self energies of the external scalar quarks evaluates to

$$\begin{aligned} \Delta_{\Phi ij}^{\text{mix}} = & \frac{G_{\Phi ij'}}{m_{\tilde{q}_{j'}}^2 - m_{\tilde{q}_j}^2} \left[c_{2\theta_{q'}} s_{2\theta_{q'}} (A_0(m_{\tilde{q}_2}^2) - A_0(m_{\tilde{q}_1}^2)) + 4c_{2\theta_{q'}} m_{q'} m_{\tilde{g}} B_0(m_{\tilde{q}_j'}^2, m_{\tilde{g}}, m_{q'}) \right] \\ & + \frac{G_{\Phi i'j}}{m_{\tilde{q}_{i'}}^2 - m_{\tilde{q}_i}^2} \left[c_{2\theta_q} s_{2\theta_q} (A_0(m_{\tilde{q}_2}^2) - A_0(m_{\tilde{q}_1}^2)) + 4c_{2\theta_q} m_q m_{\tilde{g}} B_0(m_{\tilde{q}_i}^2, m_{\tilde{g}}, m_q) \right] \end{aligned} \quad (16)$$

where $j' = 3 - j$ and $i' = 3 - i$ and A_0 the scalar one-point function [17].

The contribution from the loop diagram involving the quartic squark interaction is given by

$$\Delta_{\Phi ij}^{4\tilde{q}} = - \sum_{k,l=1,2} S_{ik}^{\tilde{q}} G_{\Phi kl} S_{lj}^{\tilde{q}'} B_0(M_\Phi^2, m_{\tilde{q}_k}, m_{\tilde{q}_l'}) \quad (17)$$

with the matrix $S^{\tilde{q}}$ defined as

$$S^{\tilde{q}} = \begin{pmatrix} c_{2\theta_q} & -s_{2\theta_q} \\ -s_{2\theta_q} & -c_{2\theta_q} \end{pmatrix}. \quad (18)$$

Finally, the gluino exchange contribution in the $\Phi\tilde{q}\tilde{q}'$ vertex reads

$$\begin{aligned} \Delta_{\Phi ij}^{\tilde{g}} = & \left\{ v_s(m_q(v_{\tilde{q}}^i v_{\tilde{q}'}^j + a_{\tilde{q}}^i a_{\tilde{q}'}^j) + m_{\tilde{g}}(v_{\tilde{q}}^i v_{\tilde{q}'}^j - a_{\tilde{q}}^i a_{\tilde{q}'}^j)) \right. \\ & \left. - a_s(m_q(v_{\tilde{q}}^i a_{\tilde{q}'}^j + a_{\tilde{q}}^i v_{\tilde{q}'}^j) + m_{\tilde{g}}(v_{\tilde{q}}^i a_{\tilde{q}'}^j - a_{\tilde{q}}^i v_{\tilde{q}'}^j)) \right\} B_0(m_{\tilde{q}_i}^2, m_{\tilde{g}}, m_q) \\ & + \left\{ v_s(m_{q'}(v_{\tilde{q}}^i v_{\tilde{q}'}^j + a_{\tilde{q}}^i a_{\tilde{q}'}^j) + m_{\tilde{g}}(v_{\tilde{q}}^i v_{\tilde{q}'}^j - a_{\tilde{q}}^i a_{\tilde{q}'}^j)) \right. \\ & \left. + a_s(m_{q'}(v_{\tilde{q}}^i a_{\tilde{q}'}^j + a_{\tilde{q}}^i v_{\tilde{q}'}^j) - m_{\tilde{g}}(v_{\tilde{q}}^i a_{\tilde{q}'}^j - a_{\tilde{q}}^i v_{\tilde{q}'}^j)) \right\} B_0(m_{\tilde{q}_j}^2, m_{\tilde{g}}, m_{q'}) \\ & + \left\{ v_s(m_q(v_{\tilde{q}}^i v_{\tilde{q}'}^j + a_{\tilde{q}}^i a_{\tilde{q}'}^j) + m_{q'}(v_{\tilde{q}}^i v_{\tilde{q}'}^j + a_{\tilde{q}}^i a_{\tilde{q}'}^j)) \right. \\ & \left. - a_s(m_q(v_{\tilde{q}}^i a_{\tilde{q}'}^j + a_{\tilde{q}}^i v_{\tilde{q}'}^j) - m_{q'}(v_{\tilde{q}}^i a_{\tilde{q}'}^j + a_{\tilde{q}}^i v_{\tilde{q}'}^j)) \right\} B_0(M_\Phi^2, m_q, m_{q'}) \\ & + \left\{ a_s m_{\tilde{g}}(v_{\tilde{q}}^i a_{\tilde{q}'}^j - a_{\tilde{q}}^i v_{\tilde{q}'}^j)(M_\Phi^2 - (m_q - m_{q'})^2) \right. \\ & - v_s m_{\tilde{g}}(v_{\tilde{q}}^i v_{\tilde{q}'}^j - a_{\tilde{q}}^i a_{\tilde{q}'}^j)(M_\Phi^2 - (m_q + m_{q'})^2) \\ & + a_s(v_{\tilde{q}}^i a_{\tilde{q}'}^j + a_{\tilde{q}}^i v_{\tilde{q}'}^j)(m_{\tilde{q}_j}^2 m_q - m_{\tilde{q}_i}^2 m_{q'} - (m_{\tilde{g}}^2 - m_q m_{q'})(m_q - m_{q'})) \\ & \left. - v_s(v_{\tilde{q}}^i v_{\tilde{q}'}^j + a_{\tilde{q}}^i a_{\tilde{q}'}^j)(m_{\tilde{q}_j}^2 m_q + m_{\tilde{q}_i}^2 m_{q'} - (m_{\tilde{g}}^2 + m_q m_{q'})(m_q + m_{q'})) \right\} \\ & \times C_0(m_{\tilde{q}_i}^2, M_\Phi^2, m_{\tilde{q}_j}^2, m_{\tilde{g}}, m_q, m_{q'}) \end{aligned} \quad (19)$$

Here, v_s and a_s denote the scalar and pseudoscalar couplings of the Higgs boson Φ to the quarks, which for H , A and H^\pm are given by

$$\begin{aligned} Hq\bar{q} : \quad & v_s = 2\sqrt{2}m_q r_1^q, \quad a_s = 0 \\ Aq\bar{q} : \quad & a_s = 2\sqrt{2}m_q(\tan\beta)^{-2I_3^q}, \quad v_s = 0 \\ H^+ t\bar{b} : \quad & v_s/a_s = 2(m_b \tan\beta \pm m_t \text{ctg}\beta) \end{aligned} \quad (20)$$

and $v_{\tilde{q}}^i, a_{\tilde{q}}^i$ are the reduced gluino–quark–squark couplings which read

$$v_{\tilde{q}}^1 = a_{\tilde{q}}^2 = \frac{1}{2}(c_{\theta_q} - s_{\theta_q}) \quad \text{and} \quad a_{\tilde{q}}^1 = -v_{\tilde{q}}^2 = \frac{1}{2}(c_{\theta_q} + s_{\theta_q}). \quad (21)$$

We have verified that these expressions agree with those given in Ref. [9] in the case of the charged Higgs boson decays into $\tilde{t}\tilde{b}$ final states.

3.2 Counterterm corrections

The counterterm corrections consist of the external squark wave-function renormalization and the renormalization of the Higgs-squark interaction. As discussed previously, this interaction involves the quark masses, the squark mixing angles and the trilinear squark couplings, and a counterterm for each of these parameters will be needed. However, the trilinear coupling can be expressed in terms of the quark and squark masses and the squark mixing angle

$$A_q = \frac{1}{m_q} s_{\theta_q} c_{\theta_q} (m_{\tilde{q}_1}^2 - m_{\tilde{q}_2}^2) - \mu (\tan \beta)^{-2I_3^q} \quad (22)$$

with the parameters μ and β not renormalized by strong interactions. Therefore, the counterterm for the trilinear coupling δA_q is fixed by the quark and squark mass counterterms δm_q and $\delta m_{\tilde{q}_i}$, and by the mixing angle counterterm $\delta \theta_q$

$$\delta A_q = \frac{m_{\tilde{q}_1}^2 - m_{\tilde{q}_2}^2}{2m_q} \left(2c_{2\theta_q} \delta \theta_q - s_{2\theta_q} \frac{\delta m_q}{m_q} \right) + s_{2\theta_q} m_{\tilde{q}_1} \frac{\delta m_{\tilde{q}_1}}{m_q} - s_{2\theta_q} m_{\tilde{q}_2} \frac{\delta m_{\tilde{q}_2}}{m_q}. \quad (23)$$

We perform the renormalization programme in the on-shell scheme where the quark and squark masses are defined as the poles of their respective propagators $\delta m_{\tilde{q}_i} = \Sigma_{ii}^{\tilde{q}}(m_{\tilde{q}_i}^2)$ and $\delta m_q = \Sigma_{ii}^q(m_q^2)$. The squark wave-function renormalization constants $\delta Z_{\tilde{q}_i}$ are defined as usual in such a way that the residues at the poles are equal to one.

Finally, as done in Ref. [18], the mixing angle counterterms are fixed by the requirement that the renormalized self energy for one of the squarks should remain diagonal, and we will choose this squark to be the lightest one. This is similar to the treatment made in Ref. [19].

The various counterterms then read

$$\begin{aligned} \frac{1}{2} \delta Z_{\tilde{q}_i} &= (m_q^2 + m_{\tilde{g}}^2 - m_{\tilde{q}_i}^2) B_0'(m_{\tilde{q}_i}^2, m_q, m_{\tilde{g}}) - B_0(m_{\tilde{q}_i}^2, m_q, m_{\tilde{g}}) + B_0(m_{\tilde{q}_i}^2, \lambda, m_{\tilde{q}_i}) \\ &\quad + 2(-1)^i s_{2\theta_q} m_{\tilde{g}} m_q B_0'(m_{\tilde{q}_i}^2, m_q, m_{\tilde{g}}) + 2m_{\tilde{q}_i}^2 B_0'(m_{\tilde{q}_i}^2, \lambda, m_{\tilde{q}_i}) \end{aligned} \quad (24)$$

$$\begin{aligned} m_{\tilde{q}_i} \delta m_{\tilde{q}_i} &= -(m_q^2 + m_{\tilde{g}}^2 - m_{\tilde{q}_i}^2) B_0(m_{\tilde{q}_i}^2, m_q, m_{\tilde{g}}) - 2m_{\tilde{q}_i}^2 B_0(m_{\tilde{q}_i}^2, \lambda, m_{\tilde{q}_i}) \\ &\quad - A_0(m_{\tilde{g}}) - A_0(m_q) + \frac{1}{2} \left[(1 + c_{2\theta_q}^2) A_0(m_{\tilde{q}_i}) + s_{2\theta_q}^2 A_0(m_{\tilde{q}_i'}) \right] \\ &\quad - 2(-1)^i s_{2\theta_q} m_{\tilde{g}} m_q B_0(m_{\tilde{q}_i}^2, m_q, m_{\tilde{g}}) \end{aligned} \quad (25)$$

$$\begin{aligned} \frac{\delta m_q}{m_q} &= - \left[2 B_1(m_q^2, m_q, \lambda) + 4 B_0(m_q^2, m_q, \lambda) + B_1(m_q^2, m_{\tilde{g}}, m_{\tilde{q}_1}) + B_1(m_q^2, m_{\tilde{g}}, m_{\tilde{q}_2}) \right] \\ &\quad + s_{2\theta_q} \frac{m_{\tilde{g}}}{m_q} \left[B_0(m_q^2, m_{\tilde{g}}, m_{\tilde{q}_1}) - B_0(m_q^2, m_{\tilde{g}}, m_{\tilde{q}_2}) \right] \end{aligned} \quad (26)$$

and

$$\delta\theta_q = \frac{1}{m_{\tilde{q}_1}^2 - m_{\tilde{q}_2}^2} \left[4m_{\tilde{g}} m_q c_{2\theta_q} B_0(m_{\tilde{q}_1}^2, m_q, m_{\tilde{g}}) + c_{2\theta_q} s_{2\theta_q} (A_0(m_{\tilde{q}_2}) - A_0(m_{\tilde{q}_1})) \right] \quad (27)$$

where again $i' = i - 3$ in eq. (25) and the functions B'_0 and B_1 are defined as

$$\begin{aligned} B'_0(q^2, m_1, m_2) &= \frac{\partial}{\partial q^2} B_0(q^2, m_1, m_2) \\ B_1(q^2, m_1, m_2) &= \frac{1}{2q^2} \left[A(m_1) - A(m_2) + (m_2^2 - m_1^2 - q^2) B_0(q^2, m_1, m_2) \right] \end{aligned} \quad (28)$$

The sum of all counterterm corrections is then given by

$$\begin{aligned} \Delta_{H^\pm ij}^{\text{CT}} &= \frac{1}{2} G_{\Phi ij} (\delta Z_{\tilde{t}_i} + \delta Z_{\tilde{b}_j}) + \frac{\partial G_{\Phi ij}}{\partial m_t} \delta m_t + \frac{\partial G_{\Phi ij}}{\partial m_b} \delta m_b \\ &\quad + \frac{\partial G_{\Phi ij}}{\partial A_t} \delta A_t + \frac{\partial G_{\Phi ij}}{\partial A_b} \delta A_b + \frac{\partial G_{\Phi ij}}{\partial \theta_t} \delta \theta_t + \frac{\partial G_{\Phi ij}}{\partial \theta_b} \delta \theta_b \end{aligned} \quad (29)$$

for the charged Higgs boson, whereas for neutral Higgs decays it reads

$$\Delta_{\Phi ij}^{\text{CT}} = \frac{1}{2} G_{\Phi ij} (\delta Z_{\tilde{q}_i} + \delta Z_{\tilde{q}_j}) + \frac{\partial G_{\Phi ij}}{\partial m_q} \delta m_q + \frac{\partial G_{\Phi ij}}{\partial A_q} \delta A_q + \frac{\partial G_{\Phi ij}}{\partial \theta_q} \delta \theta_q \quad (30)$$

Note that only the wave-function counterterm involves infrared divergences and the gluon mass λ can be set to zero everywhere except in the last term of eq. (24).

In Ref. [9], the renormalization of the quark and squark masses has been performed in the $\overline{\text{DR}}$ scheme, i.e. by subtracting the poles and the related constants in the dimensional reduction scheme; in addition there was no explicit counterterm for the trilinear squark coupling A_q . The renormalization scheme adopted here is more convenient, since the conditions we used for the masses allow for a straightforward physical interpretation.

3.3 Real corrections

Finally, the real corrections with an additional gluon in the final state need also to be included. In agreement with Ref. [9], we obtain

$$\Delta_{\Phi ij}^R = \frac{8M_\Phi^2 G_{\Phi ij}}{\lambda^{1/2}(M_\Phi^2, m_{\tilde{q}_i}^2, m_{\tilde{q}_j}^2)} \left[(M_\Phi^2 - m_{\tilde{q}_i}^2 - m_{\tilde{q}_j}^2) I_{12} - m_{\tilde{q}_i}^2 I_{11} - m_{\tilde{q}_j}^2 I_{22} - I_1 - I_2 \right] \quad (31)$$

where the phase space integrals I_{ij} and $I_{i,j}$ are defined as

$$\begin{aligned} I_{ij} &= \frac{1}{\pi^2} \int \frac{d^3 k_g}{2E_g} \frac{d^3 k_i}{2E_i} \frac{d^3 k_j}{2E_j} \frac{\delta^4(k_\Phi - k_i - k_j - k_g)}{(2k_g \cdot k_i)(2k_g \cdot k_j)} \\ I_{i,j} &= \frac{1}{\pi^2} \int \frac{d^3 k_g}{2E_g} \frac{d^3 k_i}{2E_i} \frac{d^3 k_j}{2E_j} \frac{\delta^4(k_\Phi - k_i - k_j - k_g)}{(2k_g \cdot k_{i,j})} \end{aligned} \quad (32)$$

with $k_g, k_{i,j}$ the four-momenta of the gluon and the squarks $\tilde{q}_{i,j}$. In terms of Dilogarithms, this gives

$$\begin{aligned}\Delta_{\Phi ij}^R = & \frac{2G_{\Phi ij}}{\lambda_{ij}^{1/2}} \left\{ (M_\Phi^2 - m_{\tilde{q}_i}^2 - m_{\tilde{q}'_j}^2) \left[-2 \log \left(\frac{\lambda M_\Phi m_{\tilde{q}_i} m_{\tilde{q}'_j}}{\lambda_{ij}} \right) \log \beta_0 + 2 \log^2 \beta_0 \right. \right. \\ & - \log^2 \beta_1 - \log^2 \beta_2 + 2 \text{Li}_2(1 - \beta_0^2) - \text{Li}_2(1 - \beta_1^2) - \text{Li}_2(1 - \beta_2^2) \Big] \\ & + 2 \lambda_{ij}^{1/2} \log \left(\frac{\lambda M_\Phi m_{\tilde{q}_i} m_{\tilde{q}'_j}}{\lambda_{ij}} \right) + 4 \lambda_{ij}^{1/2} + (2M_\Phi^2 + m_{\tilde{q}_i}^2 + m_{\tilde{q}'_j}^2) \log \beta_0 \\ & \left. + (M_\Phi^2 + 2m_{\tilde{q}'_j}^2) \log \beta_2 + (M_\Phi^2 + 2m_{\tilde{q}_i}^2) \log \beta_1 \right\}\end{aligned}\quad (33)$$

with $\lambda_{ij} \equiv \lambda(M_\Phi^2, m_{\tilde{q}_i}^2, m_{\tilde{q}'_j}^2)$ and

$$\begin{aligned}\beta_0 &= \frac{M_\Phi^2 - m_{\tilde{q}_i}^2 - m_{\tilde{q}'_j}^2 + \lambda_{ij}^{1/2}}{2m_{\tilde{q}_i} m_{\tilde{q}'_j}} \\ \beta_1 &= \frac{M_\Phi^2 - m_{\tilde{q}_i}^2 + m_{\tilde{q}'_j}^2 - \lambda_{ij}^{1/2}}{2M_\Phi m_{\tilde{q}'_j}}, \quad \text{and} \quad \beta_2 = \frac{M_\Phi^2 + m_{\tilde{q}_i}^2 - m_{\tilde{q}'_j}^2 - \lambda_{ij}^{1/2}}{2M_\Phi m_{\tilde{q}_i}}\end{aligned}\quad (34)$$

4. Numerical Results

In the numerical analysis of the QCD corrections we have chosen $m_t = 175$ GeV and $m_b = 5$ GeV for the top and bottom masses, $s_W^2 = 0.23$ for the electroweak mixing angle, and $\alpha_s = 0.12$ for the strong coupling constant. In Figs. 1–4, $m_{\tilde{t}_1}$ always denotes the mass of the lightest scalar top quark. The Higgs masses are fixed by $M_A = 600$ GeV, and for $\tan \beta$ we choose the value $\tan \beta = 1.6$. We will always assume that the left- and right-handed scalar masses are equal, $m_{\tilde{t}_L} = m_{\tilde{t}_R} = m_{\tilde{b}_L} = m_{\tilde{b}_R}$.

The dominating decay modes of the neutral Higgs bosons are the decays $\Phi \rightarrow \tilde{t}_i \tilde{t}_j$ into scalar top quarks. In order to visualize the effect of the QCD corrections, Figs. 2 and 3 display the decay widths of the heavy CP-even Higgs boson H and the pseudoscalar Higgs boson A into top squark pairs in Born approximation (solid lines) and including the QCD corrections for two values of the gluino mass: $m_{\tilde{g}} = 200$ GeV (dashed lines) and $m_{\tilde{g}} = 1$ TeV (dotted lines).

Fig. 2a reflects the situation for unmixed top squarks, where the choice $A_t = -\mu \cot \beta$ yields a diagonal stop mass matrix eq. (2). Fig. 2b refers to maximal mixing $\theta_t \simeq -\pi/4$ in the scalar top sector, with $A_t = 250$ GeV. $\mu = -300$ GeV is a common input for Figs. 2a,b. The decay widths are significantly larger for the case of mixing, being further increased by large QCD corrections up to nearly 50%, whereas in the unmixed case the QCD corrections decrease the Born width significantly for the major part of the \tilde{t}_1 mass range. Only close to the phase space boundary, the higher order contribution is positive.

The non-diagonal decay mode $H \rightarrow \tilde{t}_1 \tilde{t}_2$, shown in Fig. 2c for $\mu = 100$ GeV and $A_t = 150$ GeV, has a similar signature as the diagonal one in Fig. 2b, but it is suppressed

by several orders of magnitude and is thus of less interest.

For the CP-odd A boson, the non-diagonal decay is the only allowed decay mode. The width is comparable in size to that of the diagonal H boson decay. We discuss the impact of QCD corrections in terms of two examples: Fig. 3a corresponds to the parameters $\mu = -300$ GeV, $A_t = 300$ GeV. Here the corrections show a similar pattern as for the diagonal decay mode of the H with maximal mixing, Fig. 2b, having a milder dependence on the gluino mass. For other values of the μ , A_t parameters where the lowest order A width is smaller, the effect of the QCD corrections can be much more dramatic, as shown in Fig. 3b for $\mu = 100$ GeV, $A_t = 250$ GeV. Depending crucially on the gluino mass, the QCD loop contribution can be either positive ($m_{\tilde{g}} = 200$ GeV) or negative ($m_{\tilde{g}} = 1$ TeV), in both cases up to the order of 50%. The kink in Fig. 3b corresponds to the threshold $m_{\tilde{t}_2} = m_{\tilde{g}} + m_t$ in the \tilde{t}_2 wave function renormalization.

For completeness, we also present numerical results for the decay of the charged Higgs boson $H^+ \rightarrow \tilde{t}_1 \tilde{b}_1$ in order to demonstrate the impact of the QCD contributions. This decay was already studied earlier in the literature [9] using a $\overline{\text{DR}}$ renormalization scheme. As for the decay of the heavy CP-even Higgs boson H , we consider the two situations of unmixed top squarks (Fig. 4a) obtained by $A_t = -\mu \text{ctg}\beta$, $A_b = -\mu \tan\beta$, and for the case of mixing with $A_t = A_b = -100$ GeV (Fig. 4b). Both Figs. 4a,b are for $\mu = 200$ GeV. The QCD corrections are large and negative, independent of top squark mixing. They can decrease the partial decay width by almost an order of magnitude.

As seen previously the magnitude of the QCD correction strongly depends on the gluino mass. In Fig. 5a we show the dependence of the H boson decay width on $m_{\tilde{g}}$, which is treated here as an independent parameter. The two curves correspond to the case of unmixed top squarks (dotted) and stop mixing (dashed-dotted) with $A_t = 250$ GeV. The other parameters are fixed according to $\mu = -300$ GeV, $m_{\tilde{t}_L} = 150$ GeV and the solid and dashed lines indicate the respective widths in the born approximation. Whereas for the unmixed case the QCD contributions decrease the width for large $m_{\tilde{g}}$, the decay width increases with $m_{\tilde{g}}$ for the mixing case. The asymptotic dependence on $m_{\tilde{g}}$ is logarithmic; all terms linear in $m_{\tilde{g}}$ cancel in the final result. Such a logarithmic behavior has been first observed and discussed in the case of the decay of squarks into quarks and photinos [20].

The asymptotic dependence on $m_{\tilde{g}}$ can be cast into a simple form. In the notation and normalization of eqs. (7–10), the decay amplitude $G_{A\tilde{t}_1\tilde{t}_2}$ for the process $A \rightarrow \tilde{t}_1 \tilde{t}_2$ gets an additive gluino mass dependent contribution of the type

$$\begin{aligned} \Delta G_{A\tilde{t}_1\tilde{t}_2} &\simeq \frac{m_t}{\sqrt{2}} \left[(A_t - M_{LR}^t) \text{ctg}\beta - \mu \right] \frac{4\alpha_s}{3\pi} \log(m_{\tilde{g}}) \\ &= -\frac{m_t \mu}{\sqrt{2} \sin^2 \beta} \frac{4\alpha_s}{3\pi} \log(m_{\tilde{g}}) . \end{aligned} \quad (35)$$

For the H boson decays, the structure is slightly more complicated, but still very compact:

The coupling matrix $G_{H\tilde{t}\tilde{t}}$ in eq. (7) gets the following additive contribution:

$$\Delta G_{H\tilde{t}\tilde{t}} = \frac{4\alpha_s}{3\pi} \log(m_{\tilde{g}}) \Delta C_{H\tilde{t}\tilde{t}} \quad (36)$$

with the matrix

$$\begin{aligned} \Delta C_{H\tilde{t}\tilde{t}} &= 2(R^{\tilde{t}})^T C_{H\tilde{t}\tilde{t}} R^{\tilde{t}} \\ &\quad - \frac{1}{\sqrt{2}} (R^{\tilde{t}})^T \begin{pmatrix} 8r_1^t m_t^2 & m_t[(A_t + M_{LR}^t)r_1^t + \mu r_2^t] \\ m_t[(A_t + M_{LR}^t)r_1^t + \mu r_2^t] & 8r_1^t m_t^2 \end{pmatrix} R^{\tilde{t}} \end{aligned} \quad (37)$$

where $C_{H\tilde{t}\tilde{t}}$ is the matrix in eq. (8). For the special case $H \rightarrow \tilde{t}_1 \bar{\tilde{t}}_1$ we obtain:

$$\begin{aligned} \Delta C_{H\tilde{t}_1 \bar{\tilde{t}}_1} &= 2C_{H\tilde{t}_1 \bar{\tilde{t}}_1} - \frac{1}{\sqrt{2}} \left\{ 8m_t^2 r_1^t + 2s_{\theta_t} c_{\theta_t} m_t[(A_t + M_{LR}^t)r_1^t + \mu r_2^t] \right\} \\ &\simeq 2C_{H\tilde{t}_1 \bar{\tilde{t}}_1} + \frac{1}{\sqrt{2}} \left\{ 8m_t^2 \text{ctg}\beta + 2s_{\theta_t} c_{\theta_t} m_t[(A_t + M_{LR}^t)\text{ctg}\beta - \mu] \right\} \end{aligned} \quad (38)$$

From this expression, the different behaviour of the $m_{\tilde{g}}$ -dependence for the mixed and unmixed case in Fig. 5 can be qualitatively understood. It should be noted that a strong $m_{\tilde{g}}$ -dependence for intermediate values of $m_{\tilde{g}}$ is introduced via the finite part of the vertex diagram with q and \tilde{g} in the internal lines (Fig. 1b). It decouples for large $m_{\tilde{g}}$, but the decoupling is very slow.

This gluino vertex diagram is also responsible for a finite pseudoscalar decay width in case that the tree level coupling of A to $\tilde{q}_1 \tilde{q}_2$ is zero, i.e. for correlating μ and A_q such that the entries in eq. (9) vanish. Together with the counterterm from the renormalization of the trilinear coupling A_q , eq. (23), the 1-loop amplitude is ultraviolet and infrared finite and gives rise to a loop-induced finite decay width. This situation is shown in Fig. 5b for $A^0 \rightarrow \tilde{t}_1 \bar{\tilde{t}}_2$ for the parameters $A_t = \mu \tan \beta$, $\mu = \pm 100$ GeV and $m_{\tilde{t}_L} = 200$ GeV as a function of the gluino mass. The strong dependence on $m_{\tilde{g}}$ is to a large extent due to the finite part of the gluino vertex diagram, eq. (19).

5. Squark decays into Higgs Bosons

For completeness, let us also discuss the decays of scalar quarks into lighter squarks and Higgs bosons. In practice this situation can occur when there is a large mass splitting between the heaviest and the lightest top squarks where the decay

$$\tilde{t}_2 \rightarrow \tilde{t}_1 + h/A/H \quad (39)$$

can occur, and between the stop and sbottom squarks where the decays

$$\tilde{t}_2 \rightarrow H^+ + \tilde{b}_1 \quad \text{or} \quad \tilde{b}_1 \rightarrow H^- + \tilde{t}_1 \quad (40)$$

can be kinematically allowed. In the previous equation, \tilde{b}_1 is the lightest bottom squark which is identical to the left-handed \tilde{b} squark in case of no mixing in the sbottom sector;

decays of the heaviest bottom squark into neutral Higgs bosons can also be possible for large $\tan\beta$ values where the \tilde{b}_1 – \tilde{b}_2 mass splitting and the sbottom mixing angle can be large enough. These decays have been discussed at tree-level in Ref. [10] for instance.

The partial decay width of a squark \tilde{q}_i to a Higgs boson Φ and a lighter squark \tilde{q}'_j is given by a relation similar to eq. (6) but without the color factor

$$\Gamma^0(\tilde{q}_i \rightarrow \Phi \tilde{q}'_j) = \frac{G_F}{4\sqrt{2}\pi m_{\tilde{q}_i}^3} \lambda^{1/2}(m_{\tilde{q}_i}^2, M_\Phi^2, m_{\tilde{q}'_j}^2) (G_{\Phi ij})^2 \quad (41)$$

with the coupling $G_{\Phi ij}$, with $\Phi = H, A$ and H^\pm given as in section 2. The couplings of the lightest CP-even Higgs boson h to squark pairs can be obtained from those of the H boson by simply replacing α by $\alpha - \pi/2$.

The QCD corrections to the decay width are given by the Feynman diagrams shown in Fig. 1 with now \tilde{q}_i and Φ being in the initial and final state respectively. The QCD corrected decay width can be written as

$$\Gamma^1(\tilde{q}_i \rightarrow \Phi \tilde{q}'_j) = \frac{G_F}{6\sqrt{2}\pi m_{\tilde{q}_i}^3} \frac{\alpha_s}{\pi} \lambda^{1/2}(m_{\tilde{q}_i}^2, M_\Phi^2, m_{\tilde{q}'_j}^2) G_{\Phi ij} \Delta_{\Phi ij} \quad (42)$$

where, similarly to eq. (13), the correction factor $\Delta_{\Phi ij}$ is given by

$$\Delta_{\Phi ij} = \Delta_{\Phi ij}^V + \Delta_{\Phi ij}^{\text{CT}} + \Delta_{\Phi ij}^R. \quad (43)$$

The virtual corrections $\Delta_{\Phi ij}^V$ and the corresponding counterterm $\Delta_{\Phi ij}^{\text{CT}}$ are given by the same expressions as in section 3. In the real corrections, however, the role of \tilde{q}_i and the Higgs boson Φ have to be interchanged:

$$\Delta_{\Phi ij}^R = \frac{8m_{\tilde{q}_i}^2 G_0^{\Phi ij}}{\lambda^{1/2}(m_{\tilde{q}_i}^2, M_\Phi^2, m_{\tilde{q}'_j}^2)} \left[(M_\Phi^2 - m_{\tilde{q}_i}^2 - m_{\tilde{q}'_j}^2) I_{02} - m_{\tilde{q}_i}^2 I_{00} - m_{\tilde{q}'_j}^2 I_{22} - I_0 - I_2 \right] \quad (44)$$

where the functions I_{lk} [21] have arguments

$$I_{lk} \equiv I_{lk}(m_{\tilde{q}_i}, m_{\tilde{q}'_j}, M_\Phi, \lambda) \quad (45)$$

Fig. 6 shows the partial decay widths of the heaviest top squark \tilde{t}_2 into its lighter partner \tilde{t}_1 and the lightest neutral CP-even Higgs boson h (6a) and the pseudoscalar Higgs boson A (6b) as a function of the lightest top squark mass. Again, the solid lines show the tree-level decay widths, while the dashed and dotted lines show the QCD corrected widths for $m_{\tilde{g}} = 200$ GeV and $m_{\tilde{g}} = 1$ TeV, respectively. To have the \tilde{t}_2 – \tilde{t}_1 mass splitting large enough while leaving the decay rates sizeable, we relax the condition $m_{\tilde{t}_L} = m_{\tilde{t}_R}$ for the stop mass parameters. We chose $\mu = -300$ GeV, $\tan\beta = 1.6$, $A_t = 300$ GeV and $m_{\tilde{t}_R} = 500$ GeV; $m_{\tilde{t}_L}$ is then varied from 200 to 430 GeV.

In Fig. 6a, the pseudoscalar Higgs boson mass is taken to be $M_A = 400$ GeV, leading to a value $M_h \simeq 75$ GeV. This value slightly varies with $m_{\tilde{t}_L}$, since we include the large

radiative corrections in the Higgs sector which increase with m_t^4 and with the logarithm of $m_{\tilde{t}_L} m_{\tilde{t}_R}$. The $\tilde{t}_2 \rightarrow h\tilde{t}_1$ decay width is about 0.1 GeV for small \tilde{t}_1 masses and the QCD corrections increase the decay width by an amount of $\mathcal{O}(10\%)$.

In Fig. 6b, the pseudoscalar mass is chosen to be $M_A = 100$ GeV. The $\tilde{t}_2 \rightarrow \tilde{t}_1 A$ decay width is an order of magnitude larger than in the previous case, but the QCD corrections are now negative, decreasing the partial widths by 20%. Again, the kinks in Figs. 6 are due to the opening of the $\tilde{t}_2 \rightarrow t + \tilde{g}$ threshold. Above this value, this decay becomes by far the dominant one compared to the decays into Higgs bosons.

6. Conclusions

We have calculated the SUSY QCD corrections to the decays of the MSSM heavy neutral and charged Higgs bosons into scalar quark pairs, including the mixing in the squark sector. A special attention has been paid to the case of stop and sbottom decays which can be the dominant decay channels in a large area of the MSSM parameter space. The QCD corrections turn out to be quite substantial, enhancing or suppressing the decay widths in Born approximation by amounts up to 50% and in some cases more. The QCD corrections depend strongly on the gluino mass; however, for large gluino masses, the QCD correction is only logarithmically dependent on $m_{\tilde{g}}$. Contrary to the case of Higgs decays into light quarks, these QCD corrections cannot be absorbed into running squark masses since the latter are expected to be of the same order of magnitude as the Higgs boson masses.

We have also calculated the QCD corrections to the decays of heavy squarks into lighter squarks and Higgs bosons. Cases of interest are for instance the channels $\tilde{t}_2 \rightarrow \tilde{t}_1 + h/A$. The QCD corrections are at the level of a few ten percent and can enhance or suppress the tree-level decay widths. In both cases, Higgs decays into scalar quarks and squark decays into Higgs bosons, the QCD corrections are therefore important and should be included when discussing these decays.

After completion of this work, another paper appeared [22] which deals with the decays of the MSSM Higgs bosons into squark pairs. It is an extension of the earlier work [9] for the H^+ decay, but the discussion is performed also in the on-shell scheme. The difference to our renormalization scheme is only a slightly different treatment of the squark mixing angle renormalization, which results in a minor finite shift in the mixing angle counterterm. We have checked that all analytical expressions agree with ours. Numerical comparisons also show good agreement; in our case we show that the correction can strongly decrease the decay widths and determine the origin of the large corrections. The decays of heavy squarks to lighter squarks and Higgs bosons has not been discussed in Ref. [22].

Acknowledgments: We thank Roland Höpker for his collaboration in the early stage of this work.

References

- [1] For reviews on Supersymmetry see: H. P. Nilles, Phys. Rep. 117 (1985) 1;
P. Nath, R. Arnowitt and A. Chamseddine, *Applied N=1 Supergravity*, ICTP series in Theoretical Physics, World Scientific, Singapore, 1984;
Haber and G. Kane, Phys. Rep. 117 (1985) 75.
- [2] For a review on the Higgs sector of the SM and the MSSM, see J.F. Gunion, H.E. Haber, G.L. Kane and S. Dawson, *The Higgs Hunter's Guide*, Addison–Wesley, Reading 1990.
- [3] Y. Okada, M. Yamaguchi and T. Yanagida, Prog. Theor. Phys. 85 (1991) 1;
H. Haber and R. Hempfling, Phys. Rev. Lett. 66 (1991) 1815;
J. Ellis, G. Ridolfi and F. Zwirner, Phys. Lett. 257B (1991) 83;
R. Barbieri, F. Caravaglios and M. Frigeni, Phys. Lett. 258B (1991) 167.
- [4] A. Djouadi, J. Kalinowski and P. Zerwas, Z. Phys. C70 (1996) 435.
- [5] V. Barger, M. Berger and P. Ohmann, Phys. Rev. D49 (1994) 4908;
W. de Boer, A. Dabelstein, W. Hollik, W. Möhle and U. Schwickerath, hep-ph/9609202.
- [6] H. Baer, D. Dicus, M. Drees and X. Tata, Phys. Rev. D36 (1987) 1363;
J. Gunion and H. Haber, Phys. Rev. D37 (1988) 2515;
A. Djouadi, J. Kalinowski and P. Zerwas, Z. Phys. C57 (1993) 569;
J. Gunion and J. Kelly, hep-ph/9610495.
- [7] A. Djouadi, J. Kalinowski, P. Ohmann and P. Zerwas, hep-ph/9605339;
A. Bartl et al., hep-ph/9607388.
- [8] E. Brateen and J.P. Leveille, Phys. Rev. D22 (1980) 715;
M. Drees and K. Hikasa, Phys. Lett. B240 (1990) 455;
A. Mendez and A. Pomarol, Phys. Lett. B252 (1990) 461;
A. Djouadi and P. Gambino, Phys. Rev. D51 (1995) 218;
A. Djouadi, M. Spira and P.M. Zerwas, Phys. Lett. B264 (1991) 440;
M. Spira et al., Nucl. Phys. B453 (1995) 17.
- [9] A. Bartl et al., Phys. Lett. B378 (1996) 167.
- [10] A. Bartl, W. Majerotto and W. Porod, Z. Phys. C64 (1994) 499.
- [11] Particle Data Group, Phys. Rev. D54 (1996) 1.
- [12] J. Ellis and D. Rudaz, Phys. Lett. B128 (1983) 248.
- [13] J. Gunion and H. Haber, Nucl. Phys. B307 (1988) 445.

- [14] W. Siegel, Phys. Lett. B84 (1979) 193;
D. M. Capper, D.R.T. Jones, P. van Nieuwenhuizen, Nucl. Phys. B167 (1980) 479.
- [15] G. 't Hooft and M. Veltman, Nucl. Phys. B44 (1972) 189;
P. Breitenlohner and D. Maison, Commun. Math. Phys. 52 (1977) 11.
- [16] S. Martin and M. Vaughn, Phys. Lett. B318 (1993) 331.
- [17] G. Passarino and M. Veltman, Nucl. Phys. B160 (1979) 151;
G. 't Hooft and M. Veltman, Nucl. Phys. B153 (1979) 365;
G.J. Oldenborgh, Comput. Phys. Comm. 66 (1991) 1.
- [18] A. Djouadi, W. Hollik and C. Jünger, Phys. Rev. D54 (1996) 5629;
A. Djouadi, W. Hollik and C. Jünger, hep-ph/9609419, Phys. Rev. D to appear.
- [19] A. Bartl, H. Eberl, W. Majerotto, Nucl. Phys. B472 (1996) 481;
W. Beenakker, R. Höpker, T. Plehn and P.M. Zerwas, hep-ph/9610313.
- [20] K. Hikasa and Y. Nakamura, Z. Phys. C70 (1996) 139.
- [21] A. Denner, Fortschr. Phys. 41 (1993) 4.
- [22] A. Bartl et al., hep-ph/9701398.

Figure Captions

- Fig. 1:** Feynman diagrams relevant for the $\mathcal{O}(\alpha_s)$ QCD corrections to the decay of a Higgs boson Φ into scalar quark pairs. (a): gluon exchange, (b) gluino exchange, (c) mixing diagrams, (d) quartic squark interaction, (e) self-energy and vertex counterterms, (f) real corrections.
- Fig. 2:** Partial widths [in GeV] for the decays of the neutral CP-even Higgs boson into top squark pairs, $H \rightarrow \tilde{t}_i \tilde{t}_j$, as a function of $m_{\tilde{t}_1}$. The Higgs mass is fixed by $M_A = 600$ GeV and $\tan \beta = 1.6$; $\mu = -300$ GeV, $A_t = -\mu \cot \beta$ (a); $\mu = -300$ GeV and $A_t = 250$ GeV (b); $\mu = 100$ GeV and $A_t = 150$ GeV (c). The solid lines are for the partial widths in the Born approximation, while the dashed and dotted lines are for the partial widths including QCD corrections for $m_{\tilde{g}} = 200$ GeV and 1 TeV respectively.
- Fig. 3:** Partial widths [in GeV] for the decays of the neutral CP-odd Higgs boson into top squarks, $A \rightarrow \tilde{t}_1 \tilde{t}_2$, as a function of $m_{\tilde{t}_1}$. The Higgs masses are fixed by $M_A = 600$ GeV, $\tan \beta = 1.6$; $\mu = -300$ GeV and $A_t = 300$ GeV (a); $\mu = 100$ GeV and $A_t = 250$ GeV (b). The solid lines are for the partial widths in the Born approximation, while the dashed and dotted lines are for the partial widths including QCD corrections for $m_{\tilde{g}} = 200$ GeV and 1 TeV respectively.
- Fig. 4:** Partial widths [in GeV] for the decays of the charged Higgs boson into the lightest top and bottom squarks $H^\pm \rightarrow \tilde{t}_1 \tilde{b}_1$ as a function of $m_{\tilde{t}_1}$. The Higgs mass is fixed by $M_A = 600$ GeV and $\tan \beta = 1.6$; $\mu = 200$ GeV, $A_t = -\mu \cot \beta$ and $A_b = -\mu \tan \beta$ (a) and $\mu = 200$ GeV and $A_t = A_b = -100$ GeV (b). The solid lines are for the partial widths in the Born approximation, while the dashed and dotted lines are for the partial widths including QCD corrections for $m_{\tilde{g}} = 200$ GeV and 1 TeV respectively.
- Fig. 5:** Partial width [in GeV] for the decay of the neutral CP-even Higgs boson H into the lightest top squarks (a) and of the neutral CP-odd Higgs boson A into top squarks, as a function of the gluino mass. The Higgs boson masses are fixed by $M_A = 600$ GeV and $\tan \beta = 1.6$. In (a) we take $\mu = -300$ GeV, $m_{\tilde{t}_L} = 150$ GeV and $A_t = -\mu \cot \beta$ (dotted) and $\mu = -300$ GeV, $m_{\tilde{t}_L} = 150$ GeV and $A_t = 250$ GeV (dashed-dotted). The solid and dashed lines correspond to the respective born widths. In (b): A_t is fixed to make the lowest order width vanish, $A_t = \mu \tan \beta$ and the stop masses are fixed by $m_{\tilde{t}_L} = 200$ GeV; $\mu = 100$ GeV (solid) and $\mu = -100$ GeV (dashed).
- Fig. 6:** Partial decay widths of the heaviest top squark \tilde{t}_2 into \tilde{t}_1 and the lightest neutral CP-even Higgs boson h (a) and the pseudoscalar Higgs boson A (b) as a function of $m_{\tilde{t}_1}$. The solid lines show the tree-level decay widths, while the dashed and dotted lines show the QCD corrected widths for $m_{\tilde{g}} = 200$ GeV and 1 TeV, respectively. $\mu = -300$ GeV, $\tan \beta = 1.6$, $A_t = 300$ GeV and $m_{\tilde{t}_R} = 500$ GeV while $m_{\tilde{t}_L}$ is varied from 200 to 430 GeV. For the Higgs masses we take $M_A = 400$ GeV (a) and $M_A = 100$ GeV (b).

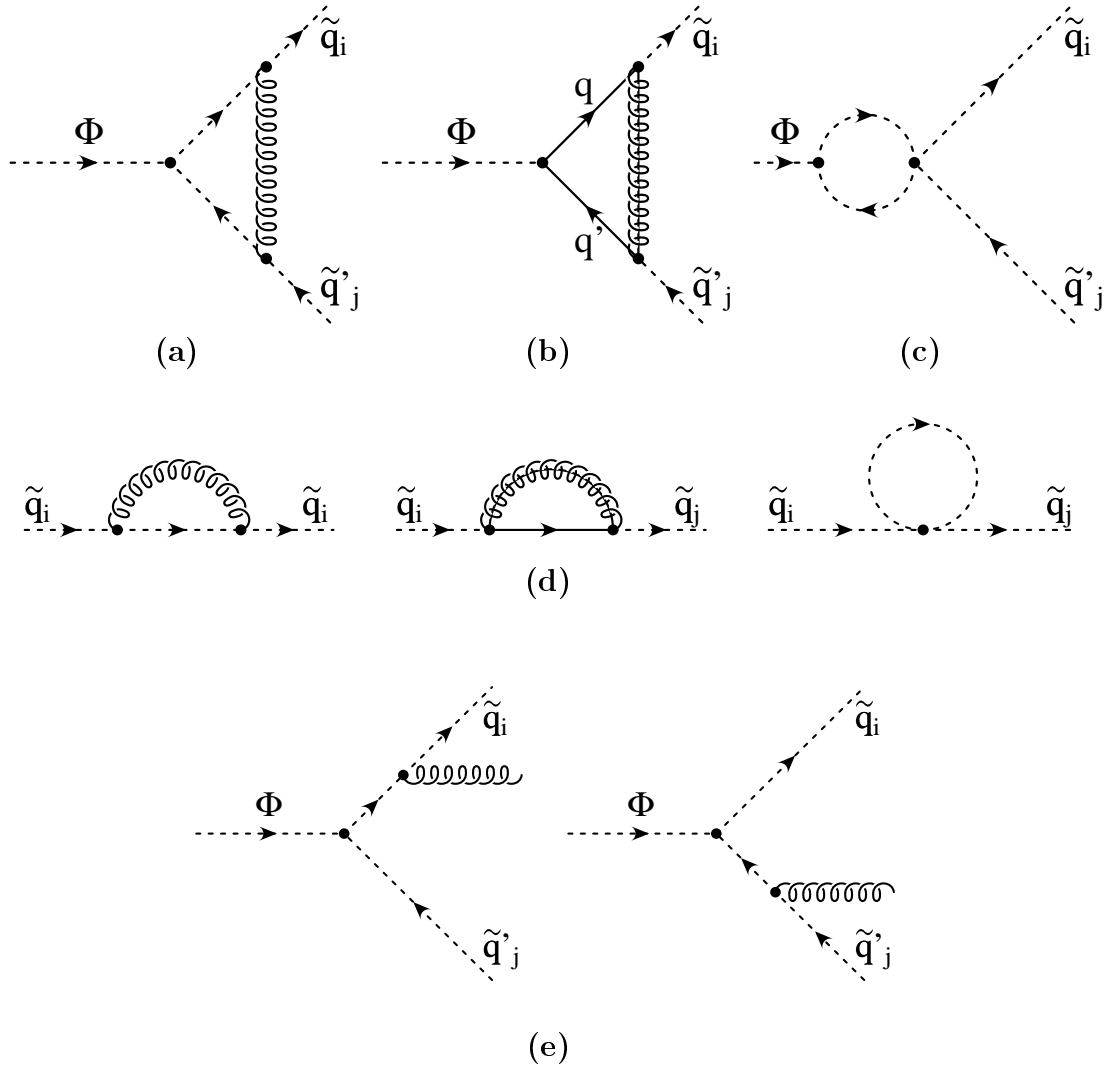
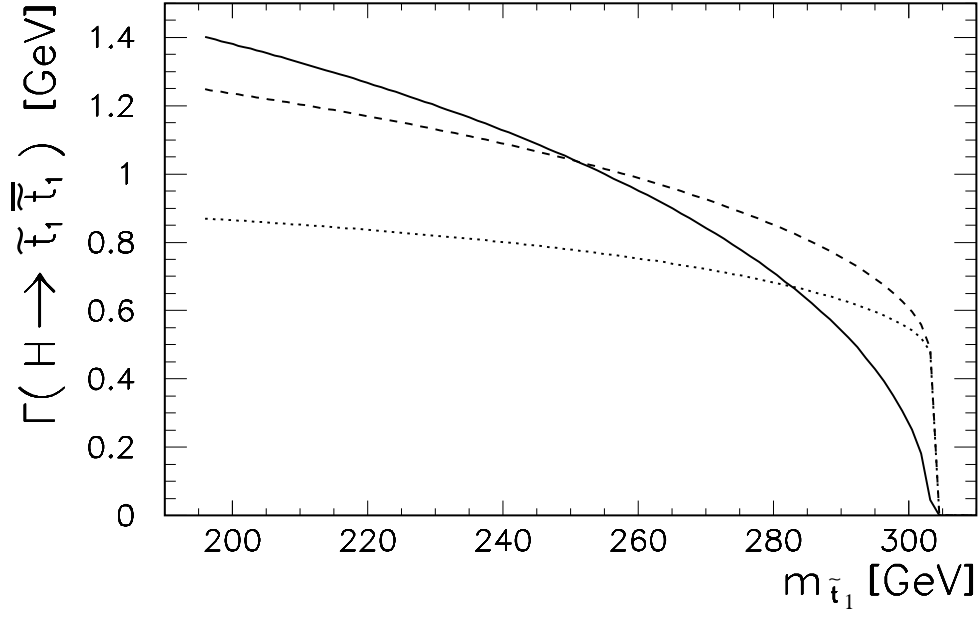
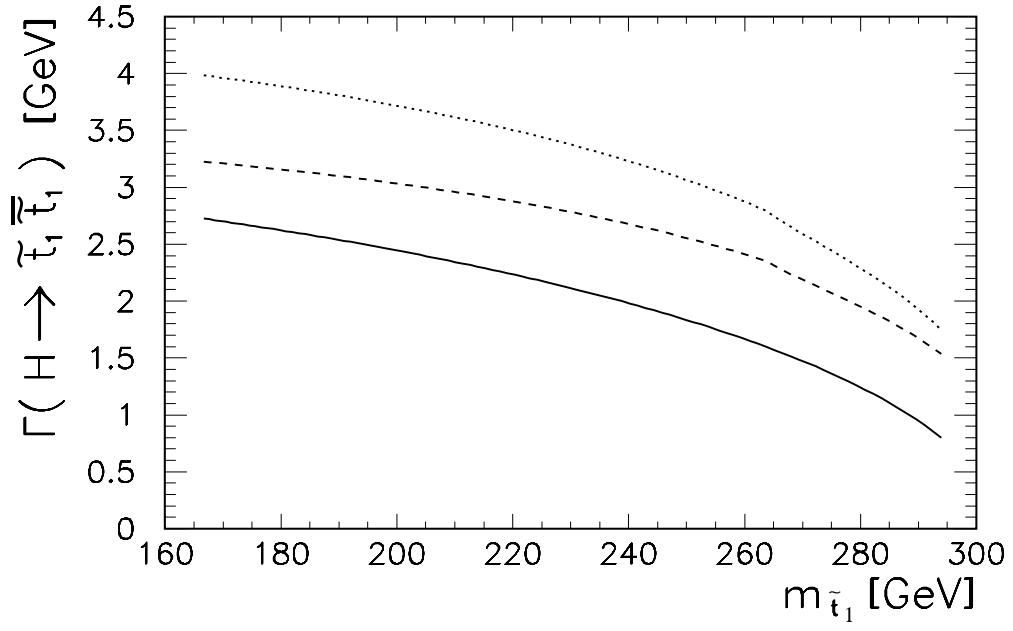


Fig. 1

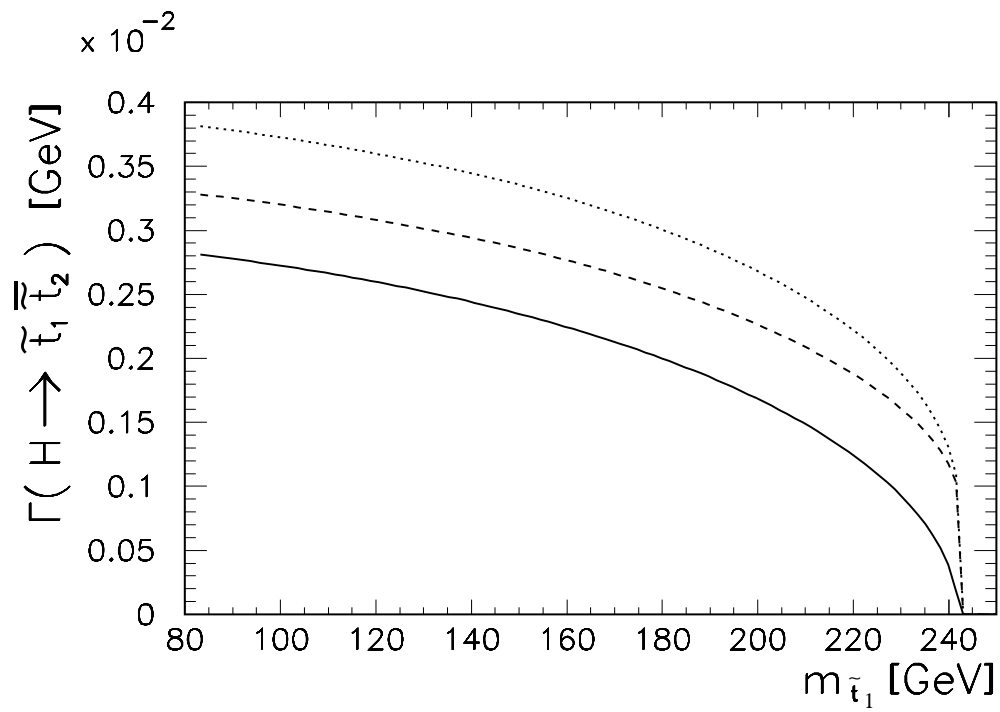


(a)



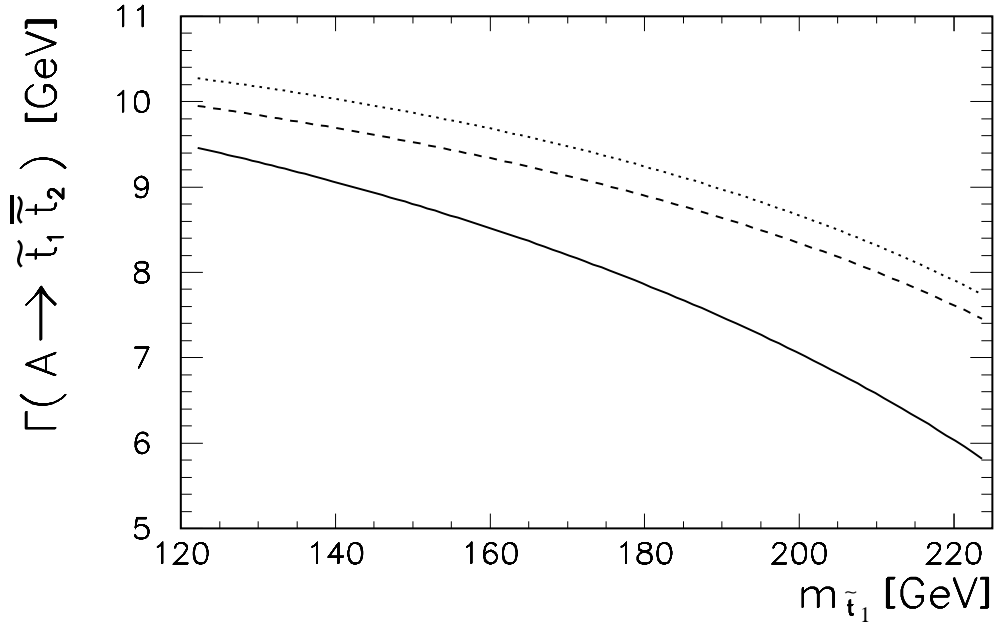
(b)

Fig. 2

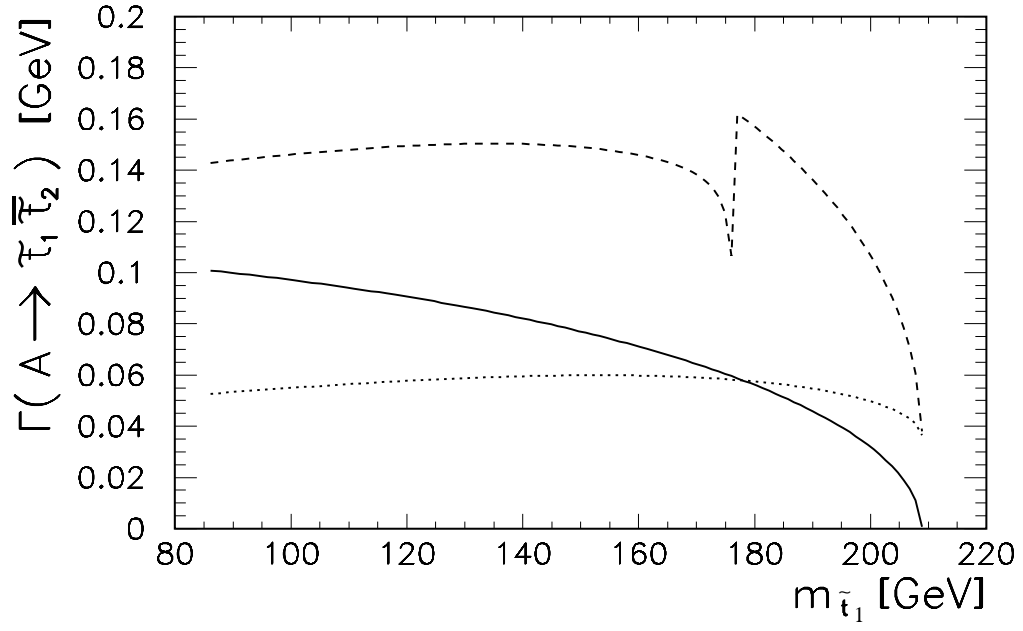


(c)

Fig. 2 (cont'd)

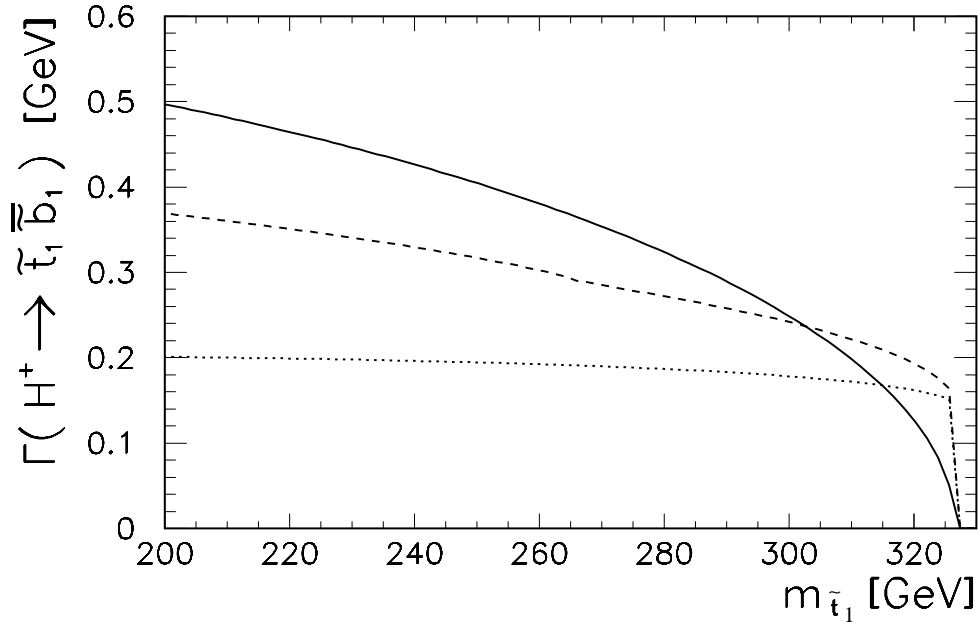


(a)

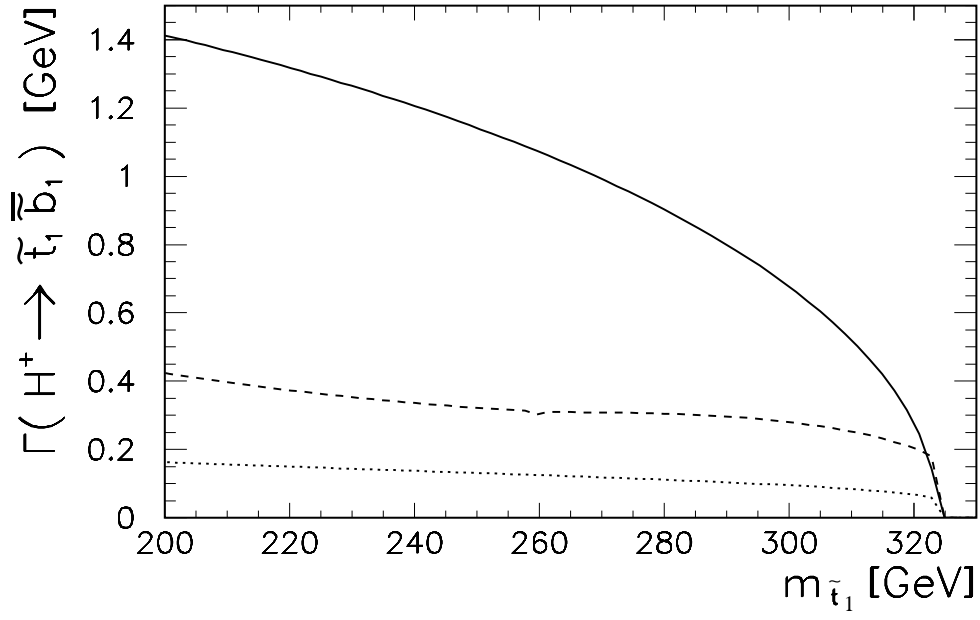


(b)

Fig. 3

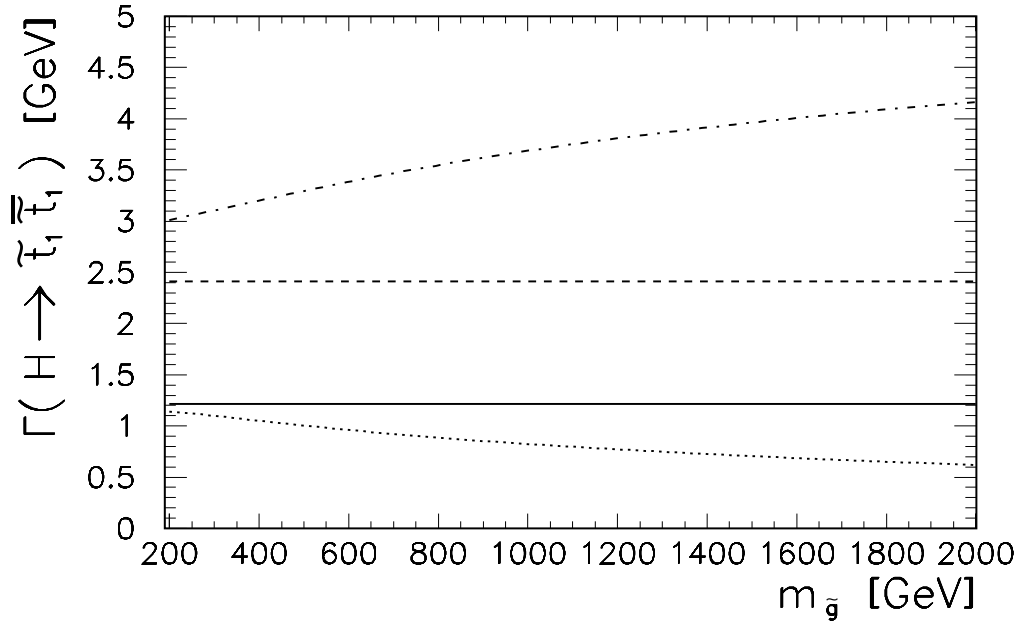


(a)

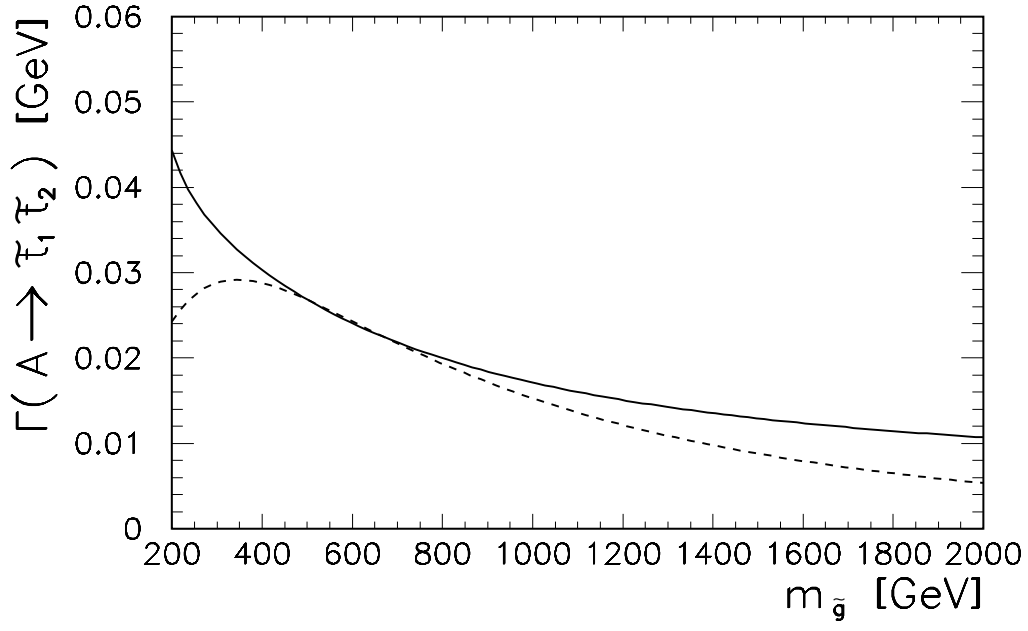


(b)

Fig. 4

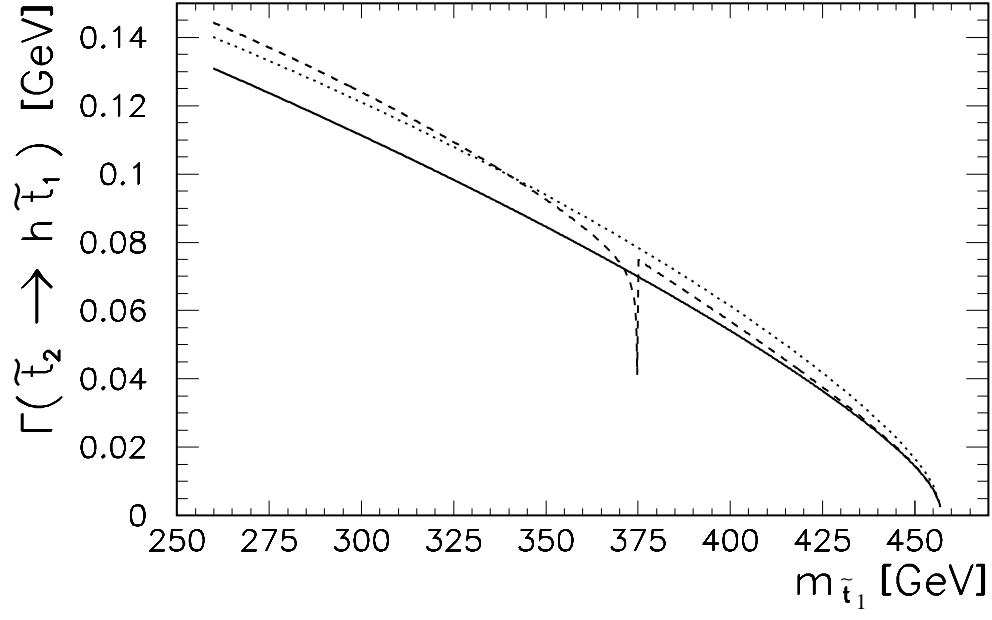


(a)

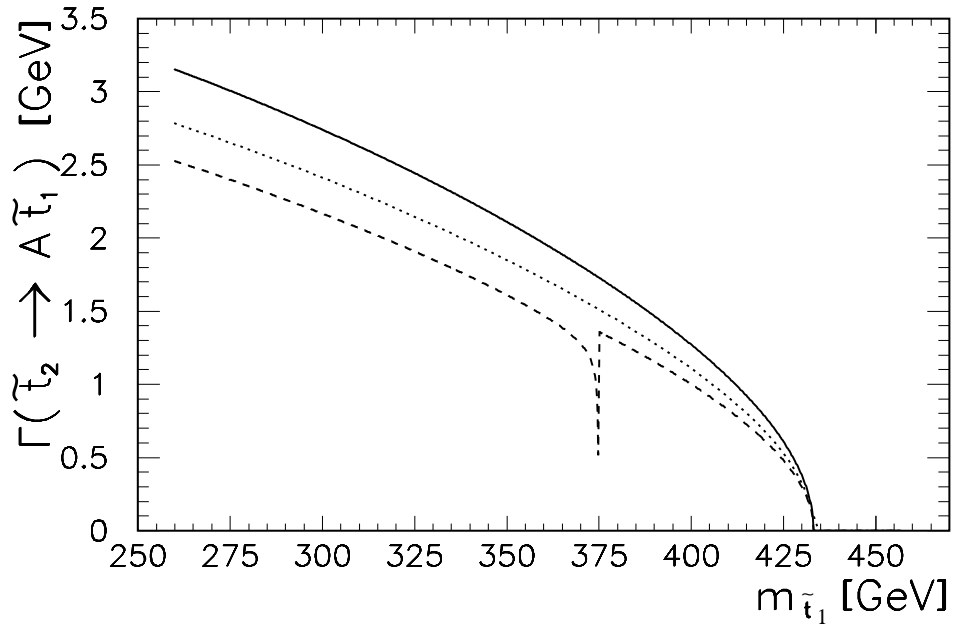


(b)

Fig. 5



(a)



(b)

Fig. 6